Improving the Colloidal Stability of PEGylated $BaTiO_3$ Nanoparticles with Surfactants

M. Taheri,[1, 2, 3, a)] S. Maaref,[3] A. Kantzas,[3] S. Bryant,[3] and S. Trudel[1, 2, b)]
[1)]*Department of Chemistry, University of Calgary, 2500 University Drive NW, Calgary, AB, Canada*
[2)]*Institute for Quantum Science and Technology, University of Calgary, 2500 University Drive NW, Calgary, AB, Canada*
[3)]*Department of Chemical and Petroleum Engineering, University of Calgary, 2500 University Drive NW, Calgary, AB, Canada*

(Dated: 10 September 2022)

Barium titanate, $BaTiO_3$, nanoparticles (NPs) have been widely used as a ferroelectric/piezoelectric/pyroelectric material in the electronic-optical ceramic industry. However, the stability of $BaTiO_3$ NP suspension are a matter of concern for their advanced applications in wet-ceramic manufacturing, imaging, and electrorheological fluids. In this study, we investigated the effect of three different surfactants (sodium dodecylbenzenesulfonate (anionic), cetyltrimethylammonium bromide (cationic), and sorbitan monooleate (non-ionic)) on the stability of PEGylated $BaTiO_3$ nanoparticles in two solvents (water and ethylene glycol) by means of dynamic light scattering, ζ potential, UV-visible spectroscopy, scanning electron microscopy, and visual observation. Our findings indicate that the anionic surfactant acted as the best stabilizer for $BaTiO_3$ nanofluids, while the cationic surfactant was the least favourable stabilizer in both water and ethylene glycol, due to the balance between attraction and repulsive forces. The results of this research provide a simple and effective approach to control and improve the colloidal stability of $BaTiO_3$ nanoparticles.

Keywords: Barium titanate, colloidal stability, cetyltrimethylammonium bromide, dispersibility, nanoparticles, surfactant, sodium dodecylbenzenesulfonate, sorbitan monooleate

I. INTRODUCTION

Biocompatible $BaTiO_3$ nanoparticles (NPs) with ferroelectric, piezoelectric and pyroelectric properties have attracted great interest for a wide range of applications in electronic-optical systems such as multilayer capacitors, sensors, and microwave dielectric ceramics,[1] or in biomedical applications including implant technology,[2,3] drug delivery,[4] cancer therapy[5] and computed tomography contrast agents.[6] Magnetic or ferroelectric nanoparticles are the most common candidates in nanofluids (*i.e.* colloidal dispersions of nanomaterials in liquids) since they are easily detectable due to their orthogonal properties not typically encountered in their surrounding medium. A key factor to successful manufacturing miniaturized electronic ceramic films via wet fabrication techniques such as colloidal processing or tape casting, is obtaining well-dispersed particles in the suspending medium.[7–9] Furthermore, the efficiency of NPs in biomedical applications strongly depends on their stability in suspension. The nanofluid stability can be drastically tuned by small variations in the solution such as pH, temperature, salinity, surfactant, NP concentration, or changes to the NPs themselves, including surface modification or tuning the particle size.[10]

Dispersing $BaTiO_3$ NPs in water is challenging since they are hydrophobic and thermodynamically unstable in solutions with pH lower than 10.[11] Ba^{2+} ions easily leach from the surface of $BaTiO_3$ particles in acidic media, leading to composition change and precipitation. Therefore, it is crucial to find an appropriate solution that stabilizes the $BaTiO_3$ NPs, forming a homogeneous dispersion. Surface coating or adding surfactants are common solutions to develop stabilized $BaTiO_3$ NPs in water or organic media.[11]

Unlike nanoparticles which have well-understood and established surface chemistry such as SiO_2[12,13] or Fe_3O_4,[14] the surface functionalization of $BaTiO_3$ NPs is still a new topic of interest. While progress is being made,[15–17] the use of surfactants remains a more straightforward approach to improving the solubility of $BaTiO_3$ NPs. Several approaches have been reported on the dispersion and stability of $BaTiO_3$ water-based dispersions, using various polymers or polyelectrolytes such as ammonium salt of poly(acrylic acid),[18–20] poly(vinyl alcohol) co-polymers with carboxylic acid group,[21] poly(aspartic acid),[22] and poly-L-lysine.[4] However, preventing aggregation of $BaTiO_3$ NPs and increasing their dispersibility are still challenging and has not yet been largely explored. Recently, we reported the development of aqueous dispersed $BaTiO_3$ NPs coated with polyethylene glycol (PEG) with high dielectric constant prepared using a simple, one-step low-temperature solution method.[23] Here, we investigate the influence of multiple surfactants to enhance the stability of these NPs in two different solvents.

Surfactants (surface active agents) are organic compounds consisting of two different moieties that are hydrophilic and hydrophobic. They are classified in four groups based on the charge existing on the hydrophilic head, *i.e.* non-ionic (without any charge), anionic (negative charge), cationic (positive charge), and zwitterionic (both negative and positive charges).[10] According to Gbadamosi *et al.*,[24] the hydrophobic tail group of a surfactants is often made of a short polymer chain, a long hydrocarbon chain, a siloxane chain or a fluo-

[a)]Electronic mail: maryam.taheri2@ucalgary.ca
[b)]Electronic mail: trudels@ucalgary.ca

rocarbon chain, while the hydrophilic head group is made of moieties such as sulfates, sulfonates, polyoxyethylene chains, carboxylates, alcohols or quaternary ammonium salts.

Dispersions will be stable when the repulsive forces between the NPs overcome the attractive forces between the same particles. Surfactants at low concentrations adsorb onto surfaces or interfaces and change the surface or interfacial free energy, usually reducing the interfacial free energy.[25] On the other hand, surfactants at high concentrations (above the critical micelle concentration) in water aggregate and form micelles. In this situation, the hydrophobic tails aggregate to the interior to reduce their contact with water, and the hydrophilic heads stay on the outer surface to maximize their contact with water.[26,27] The stability of particles in a solution depends on the balance of steric, electrostatic, hydrogen bonding, and van der Waals interactions.

The steric repulsion displays a stabilizing effect with the aid of non-ionic surfactants and polymers that can be adsorbed at the phase interface.[28] The thickness of the adsorbed layer determines the balance between the attractive and the repulsive forces, which for the polymers, depends not only on the chain length but also on its adsorption mode.[29,30] The most commonly used polymers for steric stabilization are polyethylene glycol,[31] poly(vinylalcohols),[32] poly(vinylpyrrolidones),[33,34] poly(acrylamides),[35] and poly(urethanes).[36] Non-ionic surfactants such as Brij, Tween, and Triton X-100 adsorb in a more compact mode at the NP surface compared to polymers, which create an excellent stabilizing effect.[37,38]

On the other hand, ionic surfactants can increase the surface charge of the dispersed phase. This charge provides electrostatic repulsion between NPs, preventing them from adhering to one another. The most commonly applied ionic surfactants as stabilizing agents include sodium dodecyl sulfate (SDS),[39] as a an anionic surfactant, and cetyltrimethylammonium chloride or bromide,[40] as cationic surfactants.[40,41]

There have been several investigations on the use of surfactants to control the size and agglomeration of NPs to improve their stabilization. Hwang *et al.*[42] used SDS and oleic acid to stabilize nanofluids and showed that surfactants were effective in stabilizing nanofluids by increasing the magnitude of their ζ potential. Kvitek *et al.*[43] reported the stability of uniformly sized silver NPs adding a variety of surfactants and polymers. It was found that the two surfactants of an SDS (anionic) and poly(oxyethylenesorbitane monooleate) (non-ionic) surfactants along with poly(vinylpyrrolidone) polymer prevented aggregation of silver NPs by means of both steric and electrostatic stabilization. Yi *et al.*[44] investigated the stability of nickel NP suspensions using anionic SDS, cationic cetyltrimethylammonium bromide (CTAB), and polyoxyalkalene amine derivative (Hypermer) along with xanthan gum polymer. The static stability tests and ζ potential measurements revealed the stability of nickel NPs with a combination of surfactant and polymer. Faraji *et al.*[45] showed a drastic increase in the colloidal stability of aluminum NPs in the presence of SDS surfactant during 48 hrs. Jiang *et al.*[46] studied the effect of SDS surfactant on stability of carbon nanotube (CNT) fluids and found an increase in the ζ potential of the SDS–CNTs nanofluids compared to that of the bare CNTs. They suggested that the electrostatic repulsion between the negatively charged cluster surfaces stabilized the CNT nanofluids. Wang *et al.*[47] also observed that SDS significantly increased the absolute ζ potential value in titania and alumina nanofluids by the mass fraction of 0.01 and 0.05%, respectively. Ghadimi *et al.*[48] investigated the stability of titania nano-suspensions by comparing the effect of SDS surfactant addition and ultrasonic processing. The most stable suspension was found using 0.1 wt% of SDS surfactant and 3 hrs ultrasonic bath process.

In the case of cationic surfactants, Koglund *et al.*[49] studied the structural behavior in aqueous mixtures of negatively charged silver NPs with the CTAB and dodecyltrimethylammonium chloride (DTAC). They proposed a mechanism for the stabilization of negatively charged Ag NPs in a solution of positively charged surfactants in which cluster formation of micelles in the vicinity of the particles prevented the particles from aggregating. Similarly, a recent small angle neutron scattering study on gold nano rods with CTAB proposed that the surfactants were present in a bilayer structure at the nanorod interface.[50]

In this study, we investigate the effect of different surfactants on the colloidal stability of $BaTiO_3$ dispersions. To probe the effect of charge, we selected an anionic (sodium dodecylbenzenesulfonate, SDBS), a cationic (cetyltrimethylammonium bromide, CTAB), and a non-ionic (sorbitan monooleate, SPAN 80) surfactant, shown in Scheme 1. We have carried out a comparative analysis of the stability of water and ethylene glycol (EG) based $BaTiO_3$ nanofluids by means of dynamic light scattering (DLS), ζ potential, UV-visible spectroscopy, and scanning electron microscopy (SEM). Water, EG and EG/water mixture are the most commonly-used heat transfer fluids in many industrial sectors including power generation, chemical production, air-conditioning, transportation and microelectronics.[51] EG is an organic liquid with low viscosity and volatility prevent ice formation in water by lowering the water freezing point in engine coolant fluids for the cold region, on the other hand, it increases the water boiling point used in car radiators or industrial heat exchangers.[52] The main objective of this study is a better understanding of the parameters affecting the stability of PEGylated $BaTiO_3$ NPs in aqueous and non-aqueous media, particularly, focusing on the effects of surfactant and solvent interactions.

II. EXPERIMENTAL METHODS

A. Materials

High-purity barium(II) acetylacetonate hydrate ($Ba(acac)_2 \cdot xH_2O$) and titanium diisopropoxide bis(acetylacetonate) ($(O\text{-}i\text{-}Pr)_2Ti(acac)_2$, 75 wt.% in isopropanol), polyethylene glycol ($(HO(CH_2CH_2O)_nH)$, M_w = 400), potassium hydroxide (KOH, 85%), ethylene glycol (98%), sodium dodecylbenzenesulfonate and polysorbate 80 (SPAN 80) were purchased from Sigma Aldrich. Cetyltrimethylammonium bromide was purchased from MP

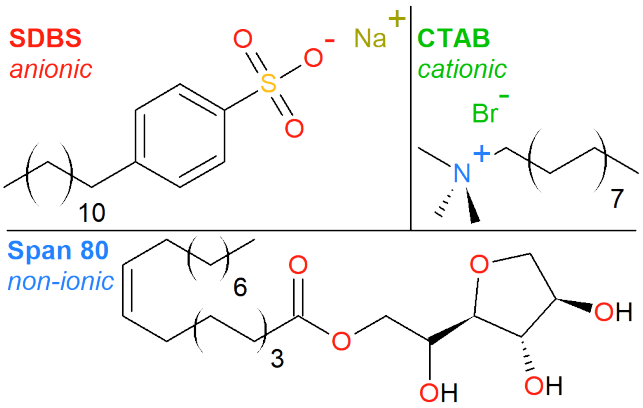

Scheme 1. Molecular structure of investigated surfactants: sodium dodecylbenzenesulfonate (SDBS, anionic), cetyltrimethylammonium bromide (CTAB, cationic) and SPAN80 (non-ionic).

Biomedical LLC. Ethanol, glacial acetic acid (99.7%) and formic acid (98%) were used for NPs' washing procedure. Deionized water was used in all experiments. All chemicals and solvents were used as-received without any further purification.

B. Nanoparticle synthesis

$BaTiO_3$@PEG (**BP**) NPs with an average particle size of 50 - 60 nm were synthesized by a low-temperature solution method using $Ba(acac)_2$ and $(O\text{-}i\text{-}Pr)_2Ti(acac)_2$ as precursors. The synthesis method and complete characterization have been reported in detail elsewhere.[23] In a representative protocol, 1 mmol of $Ba(acac)_2{\cdot}xH_2O$ powder and 1 mmol of $(O\text{-}i\text{-}Pr)_2Ti(acac)_2$ solution were mixed in 3 mL of PEG_{400} in a round-bottom flask under a nitrogen atmosphere. This solution was stirred for 30 min. Aqueous KOH (6 mL, 1.5 M) was then added to the mixture to adjust the pH of the solution to *ca.* 14; the solution is then heated to *ca.* 100 $\pm$ 5 °C, and allowed to reflux for 2 hrs. At this point, 6 mL of distilled water is added to the mixture, and maintained at 100 $\pm$ 5 °C for an additional 2 hrs. White precipitates were obtained by washing and centrifugation (6000 rpm for 10 min) two times with ethanol, followed by formic acid (1 M). Carbonate impurities were removed by washing the product with diluted (0.5 w/w %) acetic acid. The final powders were dried at 60 °C in a vacuum oven overnight, yielding $BaTiO_3$@PEG nanoparticles, **BP**.

C. Nanofluid preparation

A 200 ppm **BP** stock dispersion was prepared by mixing 20 mg of **BP** with 100 mL of solvent (deionized water (DI), or ethylene glycol (EG)), followed by 30 min of sonication. A second separate stock solution is prepared by dissolving 20 mg of surfactant in 100 mL of solvent. The surfactant stock solution is then combined to 5 mL of the **BP** stock solution, and additional solvent added to obtain the desired surfactant concentration ranging from 0 to 100 ppm, maintaining the **BP** concentration at 100 ppm in a 10-mL total volume. The final mixture was dispersed with the help of ultrasonic agitation for 30 min to obtain the stable dispersed solution. In this work, two base fluids (water and EG) and three surfactants (SDBS, CTAB and SPAN80) were studied. Table. S1 summarizes the NP and surfactant concentrations as well as type of surfactant and solvent used to prepare each nanofluid formulation.

D. Nanoparticle characterization

Hydrodynamic diameter and ζ potentials. Hydrodynamic diameter and ζ potential are recognized indicators the stability of nanofluids, measuring the size distribution of suspended NPs and their surface charge. ζ potential is the potential difference between the dispersion medium and the stationary layer of fluid attached to the dispersed particles. Generally, particles with larger surface charge (ζ potential with an a magnitude greater than 20 mV) generate sufficient repulsive forces to attain better physical colloidal stability, while colloids with smaller ζ potentials are will more readily aggregate or flocculate, due to the attractive van der Waals forces between them, resulting in a larger DLS size.[53,54] In this study, the DLS size and ζ potentials of all nanofluids were measured over time using a Malvern Zetasizer Nano ZS DLS system. Time point measurement was repeated three times at room temperature in the case of fresh nanofluids (0 hrs) and the same solutions 24 hrs later, with no disturbing.

UV-visible spectroscopy. One of the most developed, nondestructive analytical techniques to examine stability of dispersion is UV-visible spectroscopy, which measures the changes in transmitted light due to the light scattered (turbidimetry) or absorbed (absorbance) by NPs in suspension. In this technique, the extinction at a given wavelength is related to the concentration of NPs suspended in the solution through the Beer-Lambert law.[55] The extinction of **BP** nanofluids was measured at room temperature using a Mettler Toledo UV-visible Excellence (UV7) spectrometer. The spectra were collected over a wavelength range of 190-900 nm in a 1-cm cuvette. For each time-point, three sequential measurements were made for fresh nanofluids and the same solutions 24 hrs later, with no disturbing. High-temperature spectra were acquired on a Agilent Cary 5 spectrometer, equipped with w Pelletier heater.

SEM. Drops (2 μL) of fresh **BP** suspensions were cast on a silicon wafer affixed to a standard SEM sample stubs using double-sided carbon adhesive tape. **BP-DI** samples were dried in air over night while **BP-EG** samples were placed in a vacuum chamber for 15 min. All SEM images were acquired with a FEI Quanta 250 FEG field-emission SEM at an energy of 10 keV. Micrographs were analysed using the *ImageJ* freeware.[56]

III. RESULTS

Visual Test. Photographs of water-based nanofluids are presented in Fig. S1. It can be seen the solutions containing SDBS and SPAN80 in DI remain whitish-milky color over time, indicating the **BP** NP are suspended. Adding CTAB (10 - 40 ppm concentration) results in particle precipitation after 24 hrs (Fig. S1f), highlighting the low stability of these samples. Furthermore, CTAB makes more foam in the solutions at 0 hrs, compare to other surfactants. On the other hand, visual test of NP dispersions in EG (Fig. S2) confirm the better stability for all surfactants. There was no foam formation observed in the presence of CTAB. The more opaque CTAB-containing solutions including CTAB (when compared to those with SDBS and then SPAN80) is an indication of NP aggregation.

DLS and ζ Potential. In order to obtain a better understanding of the **BP** NPs stability in the presence of surfactants, the hydrodynamic diameter and ζ potential of nanofluids were measured. Fig. 1a-c shows the average hydrodynamic diameter of NPs in DI using different concentrations of SDBS, CTAB and SPAN 80, after solution preparation, and 24 hrs later. The average hydrodynamic diameter in control colloidal solution with no surfactant is around 160 nm, which slightly agglomerates after 24 hrs (180 ± 4.5 nm) (see Fig. 1a-c, grey highlight). This result is consistent with our previous study, where this observation was interpreted as aggregates comprising a few $BaTiO_3$ NPs.[23] Solutions including SDBS show a size reduction to ($\approx 105 \pm 3$ nm) for all added surfactant amounts. The hydrodynamic diameter fluctuates between 110 to 160 nm for solutions containing SPAN80, with no clear discernable trend. On the other hand, adding smaller amounts of CTAB (10 - 40 ppm) results in large agglomerates ($\approx$ 600 to 3000 nm); upon addition of more CTAB the hydrodynamic radius falls close to the control sample (130 - 170 nm).

The measured ζ potential of **BP** NPs in DI with no surfactant show a slight variation over 24 hrs ($\approx -25 \pm 6$ mV), see Fig. 1d-f. Adding SDBS and SPAN80 increases the magnitude of ζ potential, varying around an average value of -35 mV and -45 mV for colloidal mixture containing SDBS and SPAN80, respectively. The ζ potential of colloidal mixture using CTAB converts to positive value dues to the cationic nature of surfactant. The ζ potential values of less than +20 mV of fresh samples with CTAB concentrations ranging between 10 and 40 ppm confirm the low stability of the NPs, whereas more stable particles (ζ potential $\sim$ +30 mV and above) were obtained with higher concentrations (80 and 100 ppm).

As seen in Fig. 2a-c, the EG NP solutions without any surfactant show slightly larger hydrodynamic diameters ($\approx$ 250 nm) than in DI. The hydrodynamic diameter decreases in the presence of SDBS, it increases upon addition of CTAB, and remains almost constant in the presence of SPAN80. Larger hydrodynamic diameter in solutions containing CTAB after 24 hrs confirms the particles' agglomeration and low stability, while consistent and stable trends in the DLS-determined sizes for solutions containing SDBS and SPAN80 suggest higher stability.

To assess the stability of the coated NPs at high temperatures, ζ potential measurements were conducted on suspensions after 24 hours at 70 °C. The results of these experiments are summarized in Table I. In general, it can be seen that for the majority of the samples, the ζ potential is greatly decreased, and often similar to the bare NPs. Once at high temperature, the values barely change over a 24-h period.

Fig. 2d-f demonstrates the ζ potential of BP NPs in EG in different surfactant concentrations. The measured ζ potentials of colloidal solutions with SDBS show a similar trend as **BP-DI-SDBS** samples, increasing from $\approx$ -24 to -40 mV. Dispersions containing CTAB shows a decrease in the magnitude of ζ potential ($\approx$ -10 mV), confirming the stability reduction while dispersion samples containing SPAN80 present the minimum variation over time and concentration. Generally, the DLS size and ζ potential trends for colloidal solutions in both DI and EG follow the trends observed in Fig. S1 and S2 .

UV-visible spectroscopy. Fig. 3a-b shows the UV-visible extinction spectra of **BP-DI-CTAB-80** and **BP-EG-CTAB-80** nanofluids (*c.f.* Table S1) over 24 hrs. All other solutions showed similar spectrum with the maximum peak at wavelength $\approx$ 285 - 294 nm, a characteristic feature which is attributed to the Ti 3d $\leftarrow$ O2p transition in $BaTiO_3$.[57,58] Solutions with the minimum reduction in intensity have the maximum stability over time due to the minimum change in the dispersed NPs concentrations.

To examine solutions' stability, the relative maximum intensity of each sample (at the maximum extinction peak) at 24 hrs (A_{24}) compared to the initial (A_0) is plotted in Fig. 3c-d. Among the the results, **BP-DI-SDBS**, **BP-DI-SPAN80** and **BP-EG-SDBS** dispersions show no significant reduction in extinction after 24 hrs ($A_{24}/A_0 \approx 1$), while the extinction of **BP-EG-SPAN80** and **BP-EG-CTAB** decreases only lightly. On the other hand, **BP-DI-CTAB** shows the least stability (up to 80 ppm concentration). Moreover, **BP** NPs are more stable in EG than DI in the absence of surfactant. Results are in good agreement with DLS and ζ potential measurements presented above.

High-temperature UV-vis spectra were collected for two dispersions heated at 70 °C (Fig. S3, samples **BP-DI-CTAB-100** and **BP-EG-SDBS-100**. In both cases, the initial almost exactly superimpose over the spectra collected 24 hours later, indicating the dispersion are stable.

SEM. The morphology of **BP** nanofluids in 0 and 100 ppm surfactants was studied using SEM after sonicating the solutions for 30 min and drying the mixture in air (water-based fluids) or vacuum (EG-based fluids). Micrographs (see Fig. 4) indicate the agglomeration of particles in the presence of CTAB (Fig. 4c and h), compared to SDBS (Fig. 4b and g) and SPAN80 (Fig. 4d and i). Dispersibility of NPs in EG is generally better than in DI.

IV. DISCUSSION

According to the Derjaguin, Landau, Verway and Overbeek theory, the stability of nanosuspensions is determined by the sum of van der Waals attractive forces and electrostatic repulsive forces between NPs during the Brownian motion in-

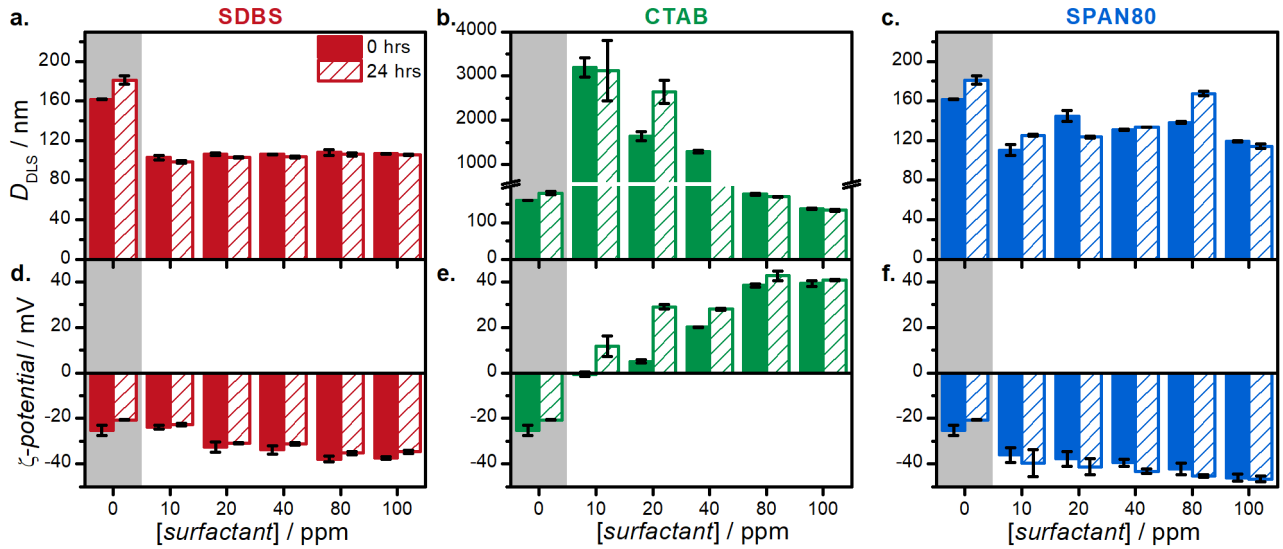

FIG. 1. Hydrodynamic diameter and ζ potential of **BP** NPs in DI water vs surfactant concentration over 24 hrs.

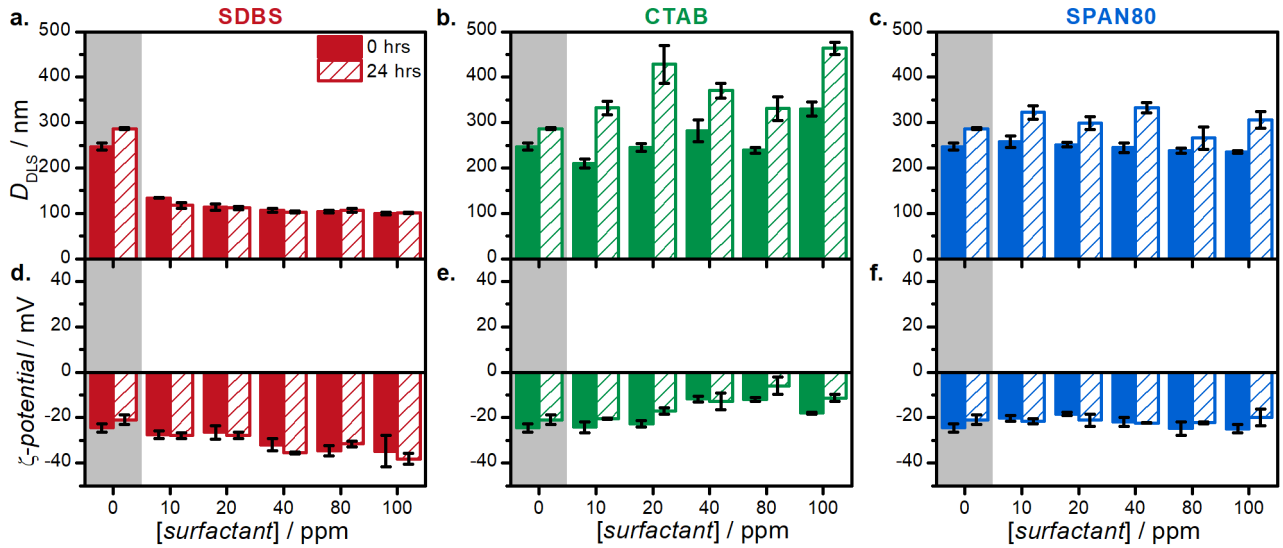

FIG. 2. Hydrodynamic diameter and ζ potential of **BP** NPs in EG vs surfactant concentration over 24 hrs.

side the fluid.[59] If the van der Waals attraction force dominates over the electrostatic repulsive force, two particles can bond together and aggregate in clusters with increased size and then precipitate due to gravity, resulting in an unstable suspension. Therefore, enhancement of repulsive forces over attractive forces can ensure stability by preventing the particle aggregation.[60]

The surfactant's role in this study is to create an effective NP coating that induces steric and/or electrostatic repulsion that can counterbalance the attractive van der Waals attractions. Based on the DLS, ζ potential, and UV-visible spectroscopy results, the anionic surfactant (SDBS) proved to be the most effective stabilizer in the dispersion of **BP** NPs among all of the tested modifiers in both water and ethylene glycol. This was attributed to the electrostatic stabilization by the aid of SDBS because of a significant increase in the absolute value of the **BP** NP surface charge reflected in the value of ζ potential in both water and EG (see Figs. 1 and 2). The electrostatic stabilization supposedly occurred by adsorption of SDBS onto the surface of NPs. This adsorption created an electrical double layer which resulted in a Coulomb repulsion force between the NPs. In other words, the surface coverage increased with an increasing in surfactant concentration, which increased the potential of the inner Helmholtz layer, leading to an increase in the charge, mutual repulsion and hence, an increase in the physical stability of the suspensions in both water and EG. Although the electrostatic stabilization is of a great importance, the steric effect of the double layer structure around NPs should also be taken into account.[61] These combined effects of SDBS resulted in the stabilization of BP NP dispersions that did not initiate any discernible aggregation over a 24-hr period.

Solvent	Temperature (°C)	Time (hr)	Surfactant	ζ potential[b] (mV)
Water	24.9	0	–	-20.5 ± 0.5
	70.0	0	–	-17.9 ± 0.4
	70.0	24	–	-16.07 ± 0.06
	70.0	0	SDBS	-23.1 ± 0.8
	70.0	24	SDBS	-20.4 ± 0.2
	70.0	0	CTAB	32.8 ± 1.1
	70.0	24	CTAB	35.2 ± 1.5
	70.0	0	SPAN80	-17.6 ± 0.6
	70.0	24	SPAN80	-18.0 ± 0.7
Ethylene glycol	25.1	0	–	-32 ± 4
	70.0	0	–	-12.1 ± 0.9
	70.0	24	–	-11.0 ± 0.8
	70.0	0	SDBS	-20.2 ± 1.7
	70.0	24	SDBS	-21 ± 2
	70.0	0	CTAB	-10.3 ± 0.3
	70.0	24	CTAB	-7.4 ± 0.5
	70.0	0	SPAN80	-13.5 ± 0.7
	70.0	24	SPAN80	-13.2 ± 0.7

[a] all suspensions contain 100 ppm $BaTiO_3$ and 100 pm surfactant (when present)
[b] average values and standard deviations based on $N = 3$ samples

TABLE I. ζ potential of NP suspension at high temperatures[a]

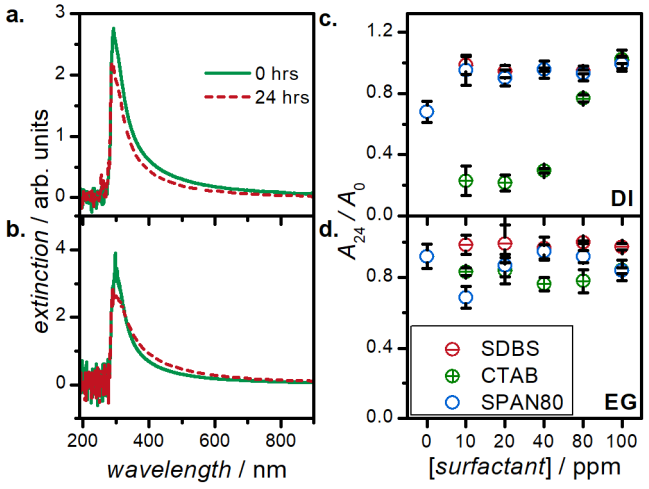

FIG. 3. a and b. UV-visible spectra of **BP-DI-CTAB-80** and **BP-EG-CTAB-80** nanofluids over 24 hrs, respectively. c and d. Surfactant concentration dependence of relative intensity (A_{24}/A_0) for **BP** NPs dispersed in DI and EG, respectively.

The results also showed that adding SPAN80 as a non-ionic surfactant increased the nanofluid stability in both water and EG, but to a lower extent than SDBS. Although a slow aggregation process was observed in the DLS measurements for SPAN 80 compared to SDBS (see Fig. 1c and 2c), no drastic increase in the size of the agglomerates was observed after 24 hrs. For particles dispersed in water, the enhancement of the aggregation stability of **BP** NPs modified by SPAN80 could be connected with a combination of both electrostatic and steric stabilization as the ζ potential of SPAN80 increased nearly two times compared to that of bare **BP** NPs. Therefore, both the electrostatic stabilization and the steric effect of the double-layer structure could be responsible for **BP** NPs stabilization in the presence of SPAN 80. However, the stability of nanofluids in EG in the presence of SPAN 80 was mostly connected to steric stabilization, as the ζ potential of the **BP** NPs remained nearly unchanged compared to bare **BP** NPs (see Fig. 2f). This steric mechanism of the stabilization could be attributed to the formation of a compact layer at the NP surface due to the adsorption of this non-ionic surfactant to **BP** NPs.

For the cationic surfactant (CTAB), the stability of **BP** NPs with a negatively charged surface occurred only after an optimum concentration in both water and EG. At low CTAB concentrations in water (especially 10 ppm and 20 ppm), the electrostatic interactions with negatively charged **BP** NPs and positively charged surfactant resulted in charge neutralization. The cancellation of the surface charge renders Coulomb reulsion inneffective, and thus leads to the formation of large aggregates (see Fig. 1b). Upon further addition of excess CTAB the surface charge of the **BP** NPs changed their sign to positive values, as seen by the ζ potential increasing drastically at concentrations above 80 ppm (see Fig. 1e). In EG, surface charge neutralization did not occur within our tested CTAB concentration range. In this solvent system, it is evident partition into the supporting phase is preferred over surface adsorption. this leads to a destabilization of the nanosuspension, as seen from increased agglomerate size (Fig. 2b) and lowered retention of NPs in solution (Fig. 3d).

As reported previously,[62–66] at low concentrations of cationic surfactants, there is a monolayer adsorption of surfactants onto the surface of negatively charged NPs. However, there will be a bilayer (chain-chain interaction of surfactants) adsorption of surfactants onto the NP surface after an optimum concentration. This bilayer formation of cationic

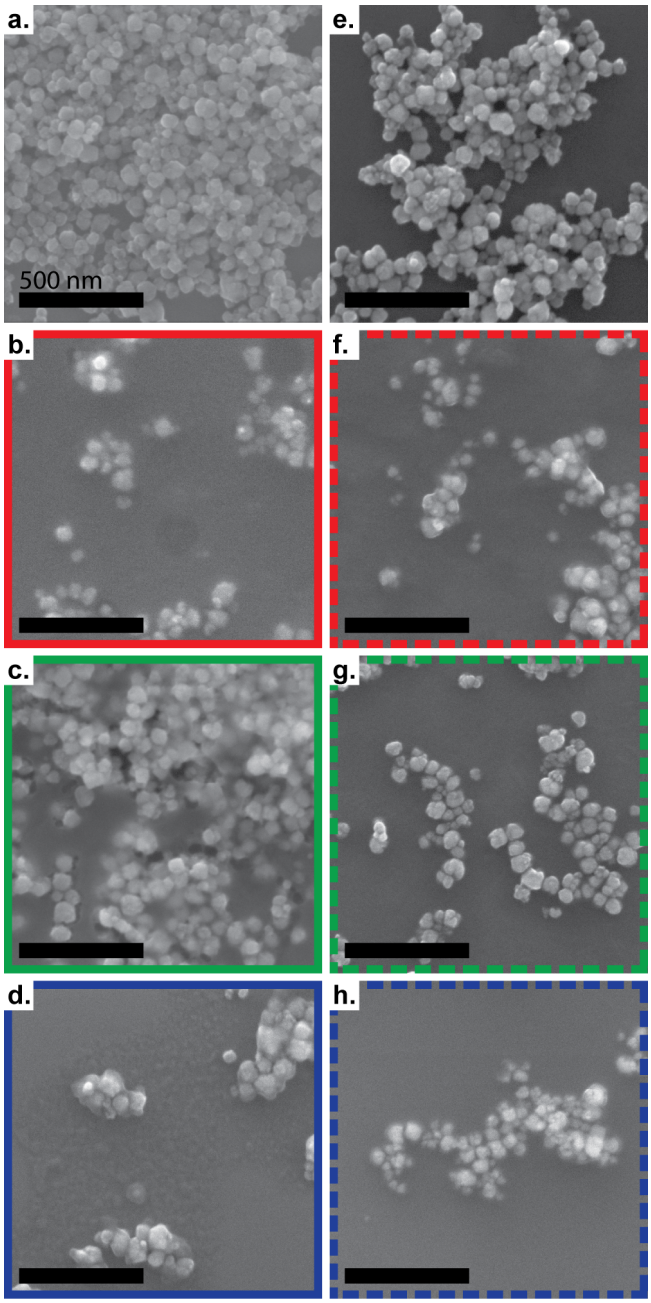

FIG. 4. SEM micrographs of $BaTiO_3$ NPs that were dispersed in water in left column: a) **BP-DI**, b) **BP-DI-SDBS-100**, c) **BP-DI-CTAB-100**, d) **BP-DI-SPAN80-100**; and samples that were disperesed in ethylene glycol in the right column e) **BP-EG**, f) **BP-EG-SDBS-100**, g) **BP-EG-CTAB-100**, h) **BP-EG-SPAN80-100**. All scale bars are 500 nm.

surfactants on the NPs at high surfactant concentration prevents NPs agglomeration due to repulsive electrostatic forces between the positively charged colloidal particles, stabilizing the dispersion in turn.[67–69] Thus, the positively charged surfactant molecules stabilize negatively charged NPs by forming a bilayer assembly surrounding the NPs.[62,63,70] In this study, although the electrostatic stabilization of **BP** NPs with CTAB occurred at concentrations above 80 ppm, a higher surfactant concentration was needed compared to SDBS and SPAN 80, which made this surfactant the least preferable candidate for **BP** NP stabilization.

To investigate the range of temperature over which these NPs can be used, their stability was investigated at elevated temperature (70 °C) via *zeta* potential measurements. In general, stability can be seen to be decreased, as indicated by lower ζ potentials. In water, NPs coated with SDBS and SPAN80 had potentials similar to those only coated with PEG. This observation most likely indicates the interaction between the surfactant and PEG-coated NPs is too weak to fully maintain coverage. A notable exception is CTAB, which retained a high positive ζ of $\sim$ +33 mV, which was stable over a 24-h period. In ethylene glycol, the CTAB and SPAN80-coated NPs had low potentials, while SDBS-coated NPs had a stable -20 mV potential, thus retaining some colloidal stability. These results are corroborated by the UV-vis spectra collected at 70 °C, which showed stable dispersions for the **BP-DI-CTAB-100** and **BP-EG-SDBS-100** samples (Fig. S3).

V. CONCLUSIONS

In summary, we studied the effect of three surfactants of SDBS, CTAB and SPAN 80 on the stability of **$BaTiO_3$-PEG** NPs in water and EG media. Among the three different surfactant modifiers, the anionic surfactant (SDBS) exhibited superior stabilization of $BaTiO_3$ NPs against aggregation in both water and EG at concentrations as low as 10 ppm as a result of electrostatic stabilization. Following SDBS, the non-ionic surfactant (SPAN 80) revealed stabilization effect at concentrations above 10$\sim$20 ppm. The mode of stabilization for the non-ionic surfactant was attributed to a combination of steric and electrostatic effects in water, while only steric stabilization is believed to be active in EG. For cationic CTAB, much higher amounts of surfactant needed to be added, as a charge neutralization and subsequent net positive charge needs to be imparted tot he NPs surface. For this reason, this makes it a less preferable surfactant for these NPs. Not all surfactants were seen to maintain colloidal stability at higher temperature, indicating a direct grafting of solubility-enhancing capping ligands to the $BaTiO_3$ NPs may be required for applications requiring stability at such temperature. This works offers a simple and effective way to stabilize dispersions of ferroelectic PEGylated $BaTiO_3$ NPs in water and polar organic solvents.

ACKNOWLEDGMENTS

We thank the University of Calgary, Natural Sciences and Engineering Research Council of Canada (NSERC, Discovery Grant and PDF), the Canada Excellence Research Chair (CERC), and the University of Calgary's Global Research Initiative in Sustainable Low Carbon Unconventional Resources funded by the Canada First Research Excellence Fund (CFREF) for supporting this research.

VI. REFERENCE

[1] M. Acosta, N. Novak, V. Rojas, S. Patel, R. Vaish, J. Koruza, G. A. Rossetti, and J. Rödel, Applied Physics Reviews **4**, 041305 (2017).
[2] H. Zarkoob, S. Ziaei-Rad, M. Fathi, and H. Dadkhah, Adv. Eng. Mater **14**, 322–329 (2012).
[3] M. Schult, E. Buckow, and H. Seitz, Curr. Dir. Biomed. Eng **2(1)**, 95–99 (2016).
[4] G. Ciofani, S. Danti, D. D'Alessandro, S. Moscato, M. Petrini, and A. Menciassi, Nanoscale. Res. Lett. **5**, 1093–1101 (2010).
[5] Y. N. Yoon, D. S. Lee, H. J. Park, and J. S. Kim, Sci. Rep. **10, 2560**, 1 (2020).
[6] R. H. Huang, N. B. Sobol, A. Younes, T. Mamun, J. S. Lewis, R. V. Ulijn, and S. O'Brien, ACS Appl. Mater. Interfaces **12**, 51135–51147 (2020).
[7] U. Paik, V. Hackley, S. Choi, and Y. Jung, Colloids Surf. A **135**, 77–88 (1998).
[8] D. Khastgir and K. Adachi, Polymer **41, 16**, 6403–6413 (2000).
[9] Z. Zheng, S. Gong, S. Cheng, D. Zhou, Y. Hu, and H. Liu, Key Eng. Mater. **368**, 469 (2008).
[10] G. Kume, M. Gallotti, and G. Nunes, J. Surfact. Deterg. **11**, 1–11 (2008).
[11] S. S. Tripathy and A. M. Raichur, J. Exp. Nanosci. **6**, 127–137 (2011).
[12] A. Liberman, N. Mendez, W. C. Trogler, and A. C. Kummel, Surf. Sci. Rep. **69**, 132 (2014).
[13] L. Zhuravlev, Colloids Surf. A Physicochem. Eng. **173**, 1 (2000).
[14] N. Zhu, H. Ji, P. Yu, J. Niu, M. U. Farooq, M. W. Akram, I. O. Udego, H. Li, and X. Niu, NANOMATERIALS **8** (2018), 10.3390/nano8100810.
[15] T. Jordan, M. A. O'Brien, C.-P. Spatarelu, and G. P. Luke, ACS Appl. Nano Mater. **3**, 2636 (2020).
[16] R. H. Huang, N. B. Sobol, A. Younes, T. Mamun, J. S. Lewis, R. V. Ulijn, and S. O'Brien, ACS Appl. Mater. Interfaces **12**, 51135 (2020).
[17] S. A. Paniagua, Y. Kim, K. Henry, R. Kumar, J. W. Perry, and S. R. Marder, ACS Appl. Mater. Interfaces **6**, 3477 (2014).
[18] J. Jean and H. Wang, J. Mater. Res. **13**, 2245 (1998).
[19] Z. G. Shen, J. Chen, H. Zou, and Y. J., J. Colloid Interface Sci. **275**, 158 (2004).
[20] J. Jean and H. Wang, J. Am. Ceram. Soc. **81**, 1589 (1998).
[21] Y. Hu, S. Gong, and D. Zhou, Mater. Sci. Eng. B, **99**, 520 (2003).
[22] X. Wang, B. Lee, and L. Mann, Colloids Surf. A. **202**, 71 (2002).
[23] M. Taheri, B. Zanca, M. Dolgos, S. Bryant, and S. Trudel, Mater. Adv. **2**, 5089–5095 (2021).
[24] A. O. Gbadamosi, R. Junin, M. Manan, A. Agi, and A. S. Yusuff, Int. Nano Lett. **9**, 171 (2019).
[25] M. Rosen, John Wiley & Sons, New York, **2ed** (1989).
[26] Y. Chevalier and T. Zemb, Rep. Prog. Phys. **53**, 279–371 (1990).
[27] C. Tanford, Wiley, New York (1980).
[28] R. J. Hunter, Foundations Colloid Sci. **xx**, 635 (2001).
[29] C. Luo, Y. Zhang, X. Zeng, Y. Zeng, and Y. Wang, J. Colloid Interface Sci. **288**, 444 (2008).
[30] D. F. Evans and H. Wennerström, *The colloidal domain: where physics, chemistry, biology, and technology meet* (Wiley-VCH, 1999).
[31] M. Popa, T. Pradell, D. Crespo, and J. M. Calderón-Moreno, Colloids Surf. A Physicochem. Eng. Asp. **303**, 184 (2007).
[32] K. S. Chou and C. Y. Ren, Mater. chem. phys. **64**, 241 (2000).
[33] H. H. Huang, X. P. Ni, G. L. Loy, K. L. Chew, C. H.and Tan, F. C. Loh, and G. Q. Xu, Langmuir **12**, 909 (1996).
[34] Z. Zhang, B. Zhao, and L. Hu, J. Solid State Chem. **121**, 105 (1996).
[35] M. Chen, L. Y. Wang, J. T. Han, J. Y. Zhang, Z. Y. Li, and D. J. Qian, J.Phy. Chem. B **110**, 11224 (2006).
[36] C. W. Chou, S. H. Hsu, H. Chang, S. M. Tseng, and H. R. Lin, Polym. Degrad. Stab. **91**, 1017 (2006).
[37] L. M. Liz-Marzán and I. Lado-Touriño, Langmuir **12**, 3585 (1996).
[38] M. H. Lee, S. G. Oh, K. D. Suh, D. G. Kim, and D. Sohn, Colloids Surf. A Physicochem. Eng. Asp. **210**, 49 (2002).
[39] F. Mafuné, J. Y. Kohno, Y. Takeda, T. Kondow, and H. Sawabe, J. Phys. Chem. B. **104**, 8333 (2000).
[40] D. Yu and V. W. W. Yam, J. Phys. Chem. B. **109**, 5497 (2005).
[41] X. Zheng, L. Zhu, A. Yan, X. Wang, and Y. Xie, J. colloid interface sci. **268**, 357 (2003).
[42] Y. Hwang, J. K. Lee, J. K. Lee, Y. M. Jeong, S. I. Cheong, Y. C. Ahn, and S. H. Kim, Powder Technol. **186**, 145 (2008).
[43] L. Kvítek, A. Panáček, J. Soukupová, M. Kolář, R. Večeřová, R. Prucek, M. Holecová, and R. Zbořil, J. Phys. Chem. C **112**, 5825 (2008).
[44] S. Yi, T. Babadagli, and H. Li, Pet. Sci. **17**, 1014 (2020).
[45] M. Faraji, R. Poursalehi, and M. Aliofkhazraei, Procedia Mater. Sci. **11**, 684 (2015).
[46] L. Jiang, L. Gao, and J. Sun, J. colloid interface sci. **260**, 89 (2003).
[47] X. J. Wang, H. Li, X. F. Li, Z. F. Wang, and F. Lin, Chin. Phys. Lett. **28**, 86601 (2011).
[48] A. Ghadimi and I. H. Metselaar, Exp. Therm. Fluid Sci. **51**, 1 (2013).
[49] S. Skoglund, E. Blomberg, I. O. Wallinder, I. Grillo, J. S. Pedersen, and L. M. Bergström, Phys. Chem. Chem. Phys. **19**, 28037 (2017).
[50] S. Gomez-Grana, F. Hubert, F. Testard, A. Guerrero-Martínez, I. Grillo, L. M. Liz-Marzán, and O. Spalla, Langmuir **28**, 1453 (2012).
[51] W. Mutuku, Asia Pac. J. Comput. Engin. **3, 1**, 1–15 (2016).
[52] G. Sekrani and S. Poncet, Appl. Sci. **8, 2311**, 1 (2018).
[53] J. Stetefeld, S. McKenna, and T. Patel, Biophys. Rev. **8**, 409–427 (2016).
[54] S. Bhattacharjee, J. Control. Release. **235**, 337–351 (2016).
[55] T. R. Ray, B. Lettiere, J. Rutte, and S. Pennathur, Langmuir. **31, 12**, 3577–3586 (2015).
[56] C. A. Schneider, W. S. Rasband, and K. W. Eliceiri, Nat. Methods **9**, 671 (2012).
[57] L. Hafid, G. Godefroy, A. El Idrissi, and F. Michel-Calendini, Solid State Commun. **66**, 841 (1988).
[58] A. U. L. S. Setyadi, Y. Iriani, and F. Nurosyid, IOP Conf. Ser.: Mater. Sci. Eng. **333**, 012035 (2018).
[59] W. Yu and H. Xie, J. Nanomater. **711**, 128 (2012).
[60] B. M. Paramashivaiah and C. R. Rajashekhar, IOP Conf. Ser.: Mater. Sci. Eng. **149**, 012083 (2016).
[61] Y. H. Chen and C. S. Yeh, Colloids Surf. A: Physicochem. Eng. Asp. **197**, 133 (2002).
[62] B. P. Binks, J. A. Rodrigues, and W. J. Frith, Langmuir **23**, 3626 (2007).
[63] Q. Lan, F. Yang, S. Zhang, S. Liu, J. Xu, and D. Sun, Colloids Surf. A: Physicochem. Eng. Asp. **302**, 126 (2007).
[64] B. P. Binks and J. A. Rodrigues, Colloids Surf. A: Physicochem. Eng. Asp. **345 (1-3)**, 195 (2009).
[65] Y. Zhu, J. Jiang, K. Liu, Z. Cui, and B. P. Binks, Langmuir **31 (11)**, 3301 (2015).
[66] Z.-G. Cui, L.-L. Yang, Y.-Z. Cui, and B. Binks, Langmuir **26 (7)**, 4717 (2010).
[67] S. Skoglund, T. A. Lowe, J. Hedberg, E. Blomberg, I. O. Wallinder, S. Wold, and M. Lundin, Langmuir **29**, 8882 (2013).
[68] J. Hedberg, M. Lundin, T. Lowe, E. Blomberg, S. Wold, and I. Odnevall Wallinder, J. Colloid Interface Sci. **369**, 193–201 (2012).
[69] Z. Sui, X. Chen, L. Wang, Y. Chai, C. Yang, and J. Zhao, Chem. lett. **34**, 100 (2005).
[70] S. Majumder, B. Naskar, S. Ghosh, C. H. Lee, C. H. Chang, S. P. Moulik, and A. K. Panda, Colloids Surf. A: Physicochem. Eng. Asp. **443**, 156 (2014).

Supplementary Material:
Improving the Colloidal Stability of PEGylated $BaTiO_3$ Nanoparticles with Surfactants

M. Taheri,[1,2,3] **S. Maaref,**[3] **A. Kantzas,**[3] **S. Bryant,**[3] **S. Trudel**[1,2]

[1]*Department of Chemistry, University of Calgary, 2500 University Drive NW, Calgary, AB, Canada;* [2]*Institute for Quantum Science and Technology, University of Calgary, 2500 University Drive NW, Calgary, AB, Canada;* [3]*Department of Chemical and Petroleum Engineering, University of Calgary, 2500 University Drive NW, Calgary, AB, Canada*

S1. SAMPLES

Sample	NPs Concentration (ppm)	Surfactant	[Surfactant] (ppm)	Solvent
BP-DI	100	N/A	0	Water
BP-DI-SDBS-10	100	SDBS	10	Water
BP-DI-SDBS-20	100	SDBS	20	Water
BP-DI-SDBS-40	100	SDBS	40	Water
BP-DI-SDBS-80	100	SDBS	80	Water
BP-DI-SDBS-100	100	SDBS	100	Water
BP-DI-CTAB-10	100	CTAB	10	Water
BP-DI-CTAB-20	100	CTAB	20	Water
BP-DI-CTAB-40	100	CTAB	40	Water
BP-DI-CTAB-80	100	CTAB	80	Water
BP-DI-CTAB-100	100	CTAB	100	Water
BP-DI-SPAN-10	100	SPAN80	10	Water
BP-DI-SPAN-20	100	SPAN80	20	Water
BP-DI-SPAN-40	100	SPAN80	40	Water
BP-DI-SPAN-80	100	SPAN80	80	Water
BP-DI-SPAN-100	100	SPAN80	100	Water
BP-EG	100	N/A	0	Ethylene glycol
BP-EG-SDBS-10	100	SDBS	10	Ethylene glycol
BP-EG-SDBS-20	100	SDBS	20	Ethylene glycol
BP-EG-SDBS-40	100	SDBS	40	Ethylene glycol
BP-EG-SDBS-80	100	SDBS	80	Ethylene glycol
BP-EG-SDBS-100	100	SDBS	100	Ethylene glycol
BP-EG-CTAB-10	100	CTAB	10	Ethylene glycol
BP-EG-CTAB-20	100	CTAB	20	Ethylene glycol
BP-EG-CTAB-40	100	CTAB	40	Ethylene glycol
BP-EG-CTAB-80	100	CTAB	80	Ethylene glycol
BP-EG-CTAB-100	100	CTAB	100	Ethylene glycol
BP-EG-SPAN-10	100	SPAN80	10	Ethylene glycol
BP-EG-SPAN-20	100	SPAN80	20	Ethylene glycol
BP-EG-SPAN-40	100	SPAN80	40	Ethylene glycol
BP-EG-SPAN-80	100	SPAN80	80	Ethylene glycol
BP-EG-SPAN-100	100	SPAN80	100	Ethylene glycol

TABLE S1. Experiment conditions of nanofluids' synthesis including $BaTiO_3$-PEG nanoparticles' concentration (BP), surfactants' type and concentration as well as type.

S2. SUPPLEMENTARY RESULTS

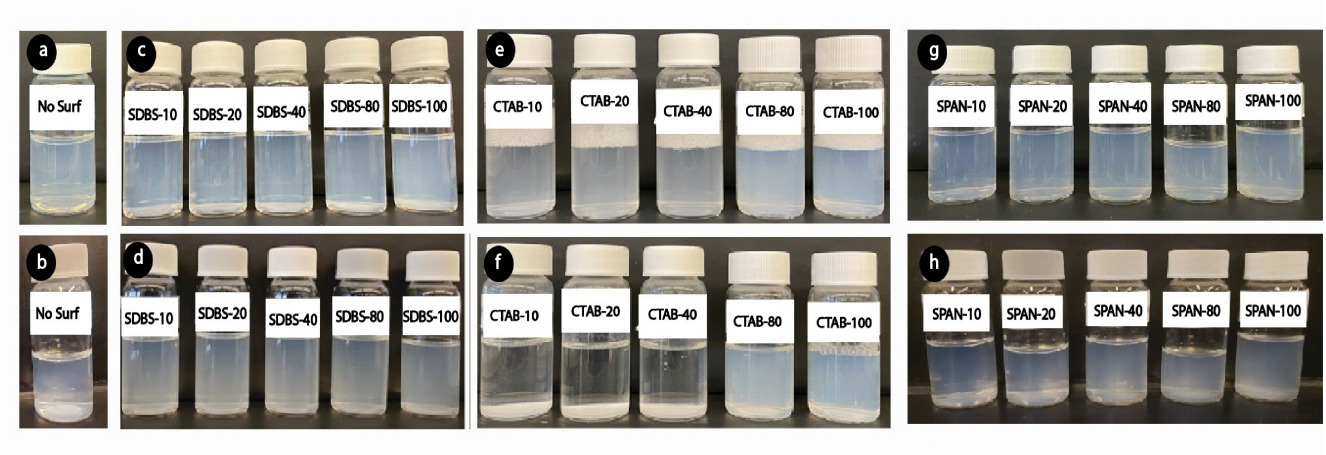

FIG. S1. Visual observations of water based nanofluid stability for BP NPs at different surfactant concentrations of: a and b. no surfactant at 0 and 24 hrs, respectively, c. and d. SDBS surfactant at 0 and 24 hrs, respectively, e. and f. CTAB surfactant at 0 and 24 hrs, respectively and g. and h. SPAN80 surfactant at 0 and 24 hrs, respectively. Concentration of surfactants were varied from 10 to 100 ppm.

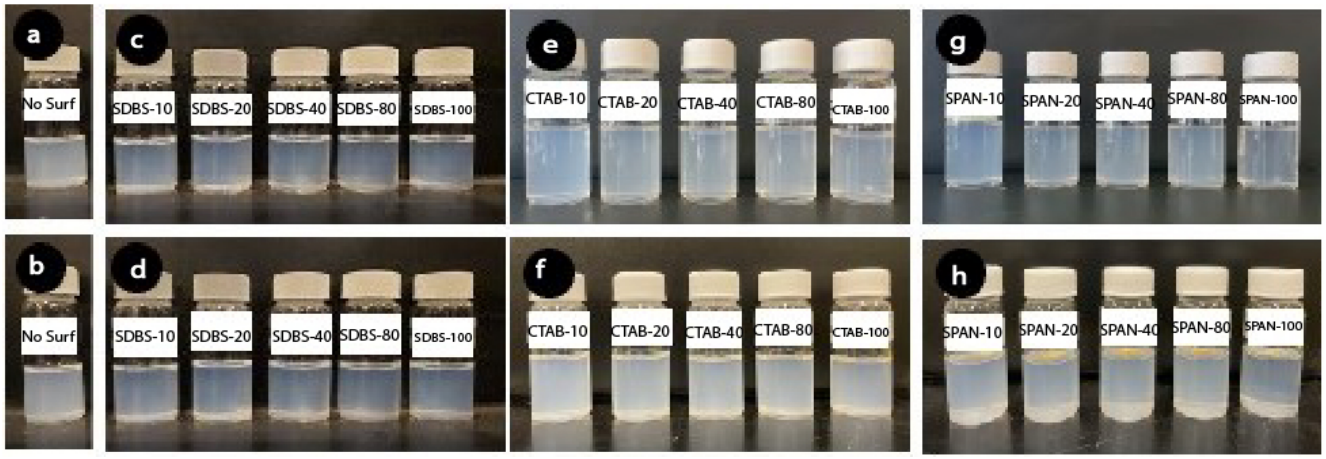

FIG. S2. Visual observations of EG-based nanofluid stability for **BP** NPs at different surfactant concentrations of: a and b. no surfactant at 0 and 24 hrs, respectively, c. and d. SDBS surfactant at 0 and 24 hrs, respectively, e. and f. CTAB surfactant at 0 and 24 hrs, respectively and g. and h. SPAN80 surfactant at 0 and 24 hrs, respectively. Concentration of surfactants were varied from 10 to 100 ppm.

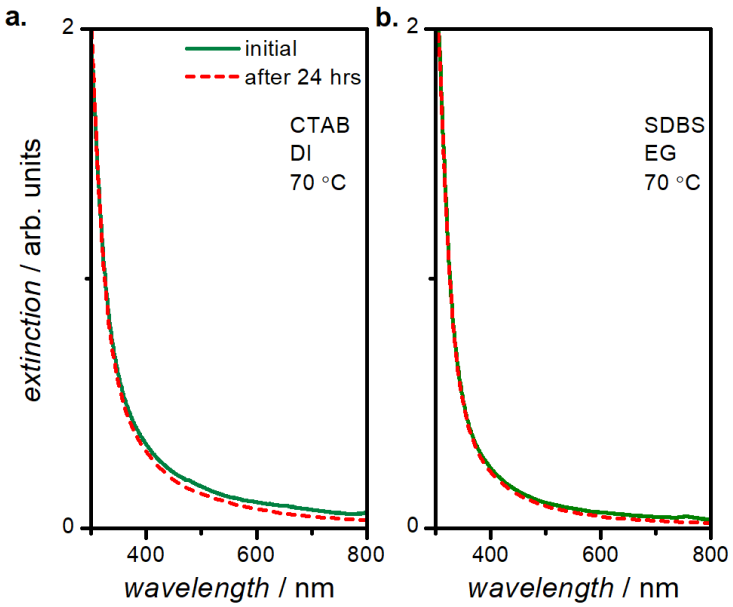

FIG. S3. UV-vis spectra of samples at 70 °C. a. CTAB-coated NPs in DI, and b. SDBS-coated NPs in EG. In both cases, the spectra show the amount of nanoparticles negligibly changed over a 24-hr period.